

# Strain history dependence of the nonlinear stress response of fibrin and collagen networks

Stefan Münster<sup>a,b,c</sup>, Louise M. Jawerth<sup>d</sup>, Beverly A. Leslie<sup>e</sup>, Jeffrey I. Weitz<sup>e,f,g</sup>, Ben Fabry<sup>b,c,1</sup>, and David A. Weitz<sup>a,d,1,2</sup>

<sup>a</sup>School of Engineering and Applied Sciences and <sup>d</sup>Department of Physics, Harvard University, Cambridge, MA 02138; <sup>b</sup>Department of Physics, University Erlangen-Nuremberg, 91052 Erlangen, Germany; <sup>c</sup>Max Planck Institute for the Science of Light, 91058 Erlangen, Germany; and <sup>e</sup>Thrombosis and Atherosclerosis Research Institute and Departments of <sup>f</sup>Medicine and <sup>g</sup>Biochemistry and Biomedical Sciences, McMaster University, Hamilton, Ontario, Canada L8L 2X2

Edited by Harry L. Swinney, University of Texas at Austin, Austin, TX, and approved May 15, 2013 (received for review December 31, 2012)

**We show that the nonlinear mechanical response of networks formed from un-cross-linked fibrin or collagen type I continually changes in response to repeated large-strain loading. We demonstrate that this dynamic evolution of the mechanical response arises from a shift of a characteristic nonlinear stress-strain relationship to higher strains. Therefore, the imposed loading does not weaken the underlying matrices but instead delays the occurrence of the strain stiffening. Using confocal microscopy, we present direct evidence that this behavior results from persistent lengthening of individual fibers caused by an interplay between fiber stretching and fiber buckling when the networks are repeatedly strained. Moreover, we show that covalent cross-linking of fibrin or collagen inhibits the shift of the nonlinear material response, suggesting that the molecular origin of individual fiber lengthening may be slip of monomers within the fibers. Thus, a fibrous architecture in combination with constituents that exhibit internal plasticity creates a material whose mechanical response adapts to external loading conditions. This design principle may be useful to engineer novel materials with this capability.**

ECM | nonlinear rheology | factor XIII | blood clot

Networks of stiff biopolymer fibers are a major component of the structural architecture of multicellular organisms; their unique material properties provide rigidity and protect structural integrity. These networks are particularly important in the extracellular matrix (ECM) where they provide mechanical support to living cells and form many of the load-carrying structures in the body. One important example is fibrin, which forms the underlying scaffold of blood clots and the provisional matrix (1). Another important example is collagen type I, the major structural constituent of all connective tissue, tendons, ligaments, and bone (2). Because the *in vivo* structure of these fiber networks is so complex, investigations of *in vitro* networks of both proteins have been used to explore their structure and unique mechanical properties, and to elucidate their underlying design principles. Interestingly, fibrin and collagen exhibit many similar features: Both proteins self-assemble into thick, hierarchically ordered, rather stiff fibers through electrostatic and hydrophobic interactions (3, 4); these fibers associate into sparse, 3D networks that possess unusual mechanical properties not seen in synthetic polymers. In both cases, these networks display highly nonlinear mechanics and stiffen significantly as the strain increases (5–8). In addition, they are both also viscoelastic: They partially store elastic energy and partially relax internal stress through dissipative processes (9–12). All of these properties are delicately influenced by the structure of the networks, by the molecular interactions between monomers, and by the addition of covalent cross-links (7, 13, 14). This creates a delicate interplay between the viscoelastic and nonlinear mechanical properties of these networks. However, the underlying nature of this interplay remains elusive; this is particularly important when a network is strained into its nonlinear regime where the material is exposed to very high stresses. In this case, little is known about how the complex viscoelastic behavior affects the internal structure and

whether this leads to a modification of the bulk mechanics. In particular, it is unclear whether the mechanical bulk response remains unchanged when the network is strained several times. In fact, it is just this repeated straining that is important for an ECM: Blood clots must withstand the pulsatory flow of blood (1). Similarly, tendons and ligaments are subjected to repeated stretch with every motion of the body; indeed, collagen-rich tissues are known to exhibit mechanics that are dependent on their loading history (15–18). However, detailed rheological measurements of pure collagen or fibrin biopolymer networks under repeated large-strain loading have never been reported. This is essential to assess whether these biopolymer networks exhibit mechanics that depend on loading history and to elucidate the interplay between viscoelastic properties and nonlinear bulk mechanics of stiff ECM biopolymer networks. This may also help determine how these structures behave in the body.

Here, we show that the mechanical response of networks formed from fibrin or collagen type I continually changes in response to repeated large-strain loading. This change shows many characteristics of weakening; however, by collapsing this response onto a master curve, we demonstrate that the dynamic evolution arises from a shift of a characteristic nonlinear stress-strain response to higher strains. Therefore, the imposed loading does not weaken the underlying matrices but instead delays the onset of the strain-stiffening response. Using confocal microscopy, we present direct evidence that this behavior does not arise from damage to the material, such as rupture of the constituent fibers or detachment of their branch points; instead, it results from persistent lengthening of the individual fibers. Furthermore, we show that covalent cross-linking of fibrin or collagen inhibits this workability of both materials, suggesting that the molecular origin of individual fiber lengthening is slip of monomers within the fibers.

## Results

**Repeated Large-Strain Loading of Fibrin Networks.** We initiate polymerization of a fibrin network by addition of 0.2 NIH units/mL human  $\alpha$ -thrombin to a 1 mg/mL fibrinogen solution at 25 °C *in situ* in a strain-controlled rheometer equipped with a plate-plate geometry. To ensure that the resulting network is completely free of covalent cross-links, we remove any traces of human factor XIII from our fibrinogen stock solution by affinity chromatography (19). We measure the nonlinear mechanical response by imposing a series of sinusoidal, large-strain oscillations of fixed amplitude while continuously recording the resulting

Author contributions: S.M., L.M.J., B.F., and D.A.W. designed research; S.M. and L.M.J. performed research; B.A.L. and J.I.W. contributed new reagents/analytic tools; S.M., L.M.J., B.F., and D.A.W. analyzed data; and S.M., L.M.J., B.F., and D.A.W. wrote the paper.

The authors declare no conflict of interest.

This article is a PNAS Direct Submission.

See Commentary on page 12164.

<sup>1</sup>B.F. and D.A.W. contributed equally to this work.

<sup>2</sup>To whom correspondence should be addressed. E-mail: weitz@seas.harvard.edu.

This article contains supporting information online at [www.pnas.org/lookup/suppl/doi:10.1073/pnas.1222787110/-DCSupplemental](http://www.pnas.org/lookup/suppl/doi:10.1073/pnas.1222787110/-DCSupplemental).



the rheometer tool by repeating the experiment and analysis using a cone–plate geometry where the strain is constant across the whole geometry of the tool (Fig. S3). Remarkably, this master curve is similar to that obtained for a virgin network when strained immediately to the highest amplitude (Fig. S14, *Inset*). Thus, the shapes of the nonlinear mechanical response of a fibrin network remain identical after repeated straining or working, demonstrating that the effect of the working of the material is to shift its nonlinear stress response to a higher strain. The shift occurs equally in both directions of the symmetrically applied sinusoidal deformations (Fig. S1). However, when the network is strained by several cyclic half-sine deformations in one direction, only that half of a full sinusoidal strain cycle is shifted, whereas the response in the other half of the cycle is unaffected (Fig. S4). Such unusual shift of the material response cannot be explained by any conventional concept of viscoelasticity. Instead, it is reminiscent of an inelastic material change that introduces an excess length into the network. This can occur through various processes: Branch points may detach (21, 22), and fibers may slide with respect to one another (23), may bundle (24), or may rupture.

**Confocal Imaging of a Fibrin Network Held Under Shear.** To elucidate the nature of this lengthening, we polymerize a fluorescently labeled fibrin network between two parallel glass plates on a confocal microscope and directly image the network structure while we perform a strain hold experiment: We impose a sudden shear deformation of a strain of 0.7 by translating the top plate and acquire a full 3D image every minute for 1 h; thereafter, we release the shear by returning the plate to its initial, 0-strain position and immediately acquire another 3D image. The unstrained, virgin fibrin network is composed of sparse, randomly oriented fibers, which are initially nearly straight (Fig. 2A). Upon being sheared, the deformation of individual fibers depends on their orientation in the network: Fibers stretch and their length increases when oriented in the direction of shear; whereas, rather than being compressed, they buckle when oriented perpendicular to the direction of shear as highlighted by the red and blue lines, respectively, in Fig. 2A. When we perform a similar strain hold experiment with the rheometer, we find that the network stress decreases significantly, to less than 20% of its initial value, over the course of 1 h (Fig. S5A). Surprisingly, however, when we examine the evolution of the structure of the network under shear, there are no obvious changes in the sheared structure visible during the entire period; instead the network appears completely static (Movie S1): We observe no rupture of

individual fibers or branch points, no detachment of fibers from the plates, and no significant sliding of fibers with respect to one another. Thus, network stress is relaxed, yet the network structure remains fully static. Therefore, stress relaxation must occur within the fibers themselves; this is consistent with atomic force microscopy experiments on single fibers (25).

When the imposed strain is removed, the branch points of the network return approximately to their initial position; however, the shapes of the fibers differ significantly from their initial state: Fibers that were buckled under shear return relatively straight, whereas fibers that were stretched under shear now appear buckled and curved as shown in Fig. 2A and Movie S2. This buckling suggests that stretched fibers do not fully retract to their original rest length but instead become longer.

To confirm that fibers do indeed lengthen after they have been temporarily stretched, we image an individual fibrin fiber suspended perpendicularly over a microchannel (26) and repeatedly stretch it with a glass capillary pulled to a 1- $\mu\text{m}$  diameter tip and mounted onto a micromanipulator. The initially straight fiber is stretched laterally along the channel until its length is increased by  $\sim 75\%$ . After holding this deformation for 5 s, we release the fiber and then repeat this procedure 15 times in 10-s intervals. After each stretch, the shape of the fiber becomes increasingly bowed as seen in Fig. 2B. This demonstrates that the fiber rest length does indeed increase when it is stretched.

**Microscopic Origin of the Bulk Response.** We can use these observations to understand the bulk network behavior on an individual-fiber basis: When the network is sheared, each fiber of the subset oriented in the direction of shear is stretched, putting it under tension (Fig. 3A, I–II). However, the rest lengths of these fibers increase over time, thereby relaxing most of this tension (Fig. 3A, III). As the applied strain returns to zero, the system returns to its initial position, putting the lengthened fibers under compression; instead of shortening to their original rest lengths they buckle and remain lengthened (Fig. 3A, IV). Thus, when the fibrin network is sheared again, these lengthened fibers do not contribute to the total network shear stress until their undulations are pulled out and they become taut (Fig. 3A, V–VI). This delayed engagement of these fibers leads to the observed shift of the shear response of the entire system to higher strains. The amount fibers lengthen during each cycle is a fraction of their relative stretch; therefore, as the rest length of these fibers increases, their successive relative stretch becomes less, leading to the asymptotic approach to their maximum increase in length.

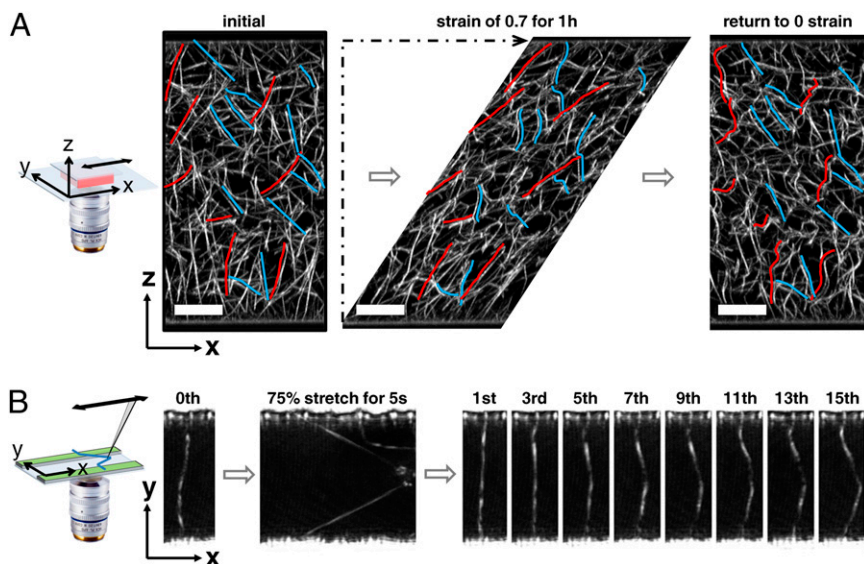


**Fig. 2.** Structural changes of an un-cross-linked fibrin network held under shear deformation, and the effect of repeated stretching of an individual fibrin fiber. (A) A fluorescently labeled 1 mg/mL fibrin network free of covalent cross-links is polymerized in a custom-built shear cell consisting of two parallel glass plates. Its 3D network structure is imaged before (*Left*), during (*Center*), and after (*Right*) a shear deformation of a strain of 0.7 is applied for 1 h by translating the top plate horizontally while the bottom stays stationary. The colored lines highlight fibers in the direction of shear (right of red lines) and perpendicular to the direction of shear (left of blue lines). All images are  $x$ - $z$  projections of a volume spanning 15  $\mu\text{m}$  in the  $y$  direction. (Scale bar: 20  $\mu\text{m}$ .) (B) An individual fibrin fiber suspended perpendicularly over a 20- $\mu\text{m}$ -wide micropatterned channel is stretched 15 times for 5 s to 175% of its original length with a pulled glass capillary. With ongoing cycles, the fiber appears increasingly bowed, indicating that it becomes successively longer.

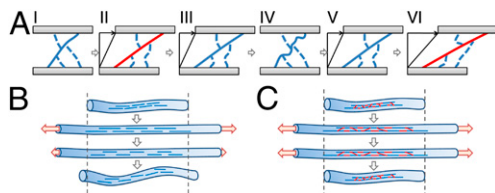


**Fig. 3.** Lengthening of viscoelastic fibers due to stretching followed by buckling. (A) (I) Fibers oriented in the direction of shear (solid line) and fibers oriented perpendicular to it (dashed lines) behave differently when the bulk is sheared. (II) Upon shear, fibers in the direction of shear are stretched, putting them under tension (red line), whereas fibers perpendicular to it buckle. (III) The tension within the stretched fibers relaxes quickly due to internal viscoelastic processes, leading to an increase of their rest lengths. (IV) Upon return of the bulk deformation to the initial 0-strain position, lengthened fibers remain so, because they do not become compressed, but instead buckle. (V) When the network is sheared again, the lengthened fibers do not contribute to the bulk shear stress until they are pulled taut. (VI) Once the shear amplitude exceeds those of previous cycles, fibers contribute to the shear stress as before, which accounts for the observed shift of the bulk stress response to higher strains. (B) When an un-cross-linked fiber is put under tension, slip of protofibrils (blue lines) leads to a strong relaxation of the internal stress and causes the rest length of the fiber to increase. (C) By contrast, in a fiber fully cross-linked, adjacent protofibrils are covalently bound to one another (red links) and do not slip under tension leading to a suppressed relaxation; therefore, the fiber retains its initial rest length upon stress release.

Thus, for a constant strain amplitude, the successive shift of the stress response slows as does the decrease of the maximum stress. However, when the strain amplitude is increased, fibers are again stretched beyond the increased length to which they have been worked, and, hence, the lengthening and corresponding shift in the stress response begins anew. Moreover, once the lengthened fibers are pulled taut, the stress-strain response of the network is again similar to the virgin network. This provides a fiber-level account of the stress-strain response behavior of the bulk and its scaling, as observed in Fig. 1. For symmetrically applied shear deformations, the fibers of each of the two orthogonal subpopulations are lengthened during the respective half-cycles and, hence, the response of the fibrin network shifts in a similar fashion in each strain direction. By contrast, when the network is sheared asymmetrically in one direction, only fibers in the subpopulation that is stretched are lengthened; those in the subpopulation of orthogonal fibers remain unaltered. This explains our observation that an asymmetrically worked network displays a shift of its mechanical response only in the direction that it is worked, while its properties remain unaltered in the other direction.

**Effect of Covalent Cross-Linking.** The stress relaxation and lengthening of the fibrin fibers under stretch can be explained by their microscopic nature: Fibrin fibers are self-assembled arrays of

fibrin protofibrils whose mechanical properties, as well as their interaction with each other, determine the mechanics of the fibers (1, 13). Slippage between protofibrils or the breaking of knob-hole bonds drive stress relaxation in fine fibrin clots (5, 27, 28) and may occur within the fibers themselves in coarse clots (29) (Fig. 3B). Furthermore, the dissociation of oligomers (30) could also contribute to stress relaxation and fiber lengthening. All of these mechanisms are inhibited with the introduction of physiologically important covalent cross-links by activated factor XIII (factor XIIIa), which catalyzes the formation of covalent bonds that not only link fibrin monomers within protofibrils to each other but also link adjacent protofibrils (30, 31). If protofibrils neither slip nor break, the fibers will not lengthen and the stress response of the system should not shift (Fig. 3C). We therefore hypothesize that a fibrin network that is covalently cross-linked by factor XIIIa will show a decreased shift of the stress response under cyclic loading.

To test this hypothesis, we repeat the same measurement protocol on an equivalent fibrin network that has not been depleted of factor XIII and, hence, is completely cross-linked (Fig. S6). In this case, the stress-strain response is unchanged with subsequent cycles at constant amplitude and the data loops fully overlap each other (Fig. 4A, same colors). Moreover, upon increase of the strain amplitude, the loading branches of each stress-strain response exactly follow the same trace, whereas the unloading branches return at correspondingly higher strains (Fig. 4A, different colors). These data demonstrate that the onset of nonlinearity of the cross-linked system always occurs at the same strain, regardless of the previous loading history of the material. This confirms our hypothesis that covalent cross-linking of the system inhibits the shift of the bulk mechanics to higher strains (Fig. 4A, *Inset*); moreover, these data suggest that, in the absence of covalent cross-links, the nonpermanent coupling of monomers is the origin of the observed change of the mechanical properties of the un-cross-linked fibrin network.

**Similarity with Collagen Networks.** Self-assembly of monomers into fibers is a common strategy not only inherent to fibrin networks but shared by many other biopolymers. Fibers of other proteins constructed in such a way may also be susceptible to slip of their monomers with respect to one another and, thus, may be susceptible to working of their bulk response. To ascertain whether the mechanical behavior reported here is limited to fibrin or shared by other biopolymers of this class, we repeat our measurements on another important example of a biopolymer network that is composed of nonpermanently coupled, self-assembled fibers: collagen type I (2, 3). We use a similar cyclic-strain protocol on a reconstituted network of 0.9 mg/mL collagen type I, polymerized at 25 °C in situ (Fig. 1D, *Upper Inset*). Like fibrin, collagen is viscoelastic and exhibits highly nonlinear loading and unloading cycles, with each oscillation featuring closed loops with sharp upturns (Fig. 1D and *Lower Inset*). However, unlike fibrin,

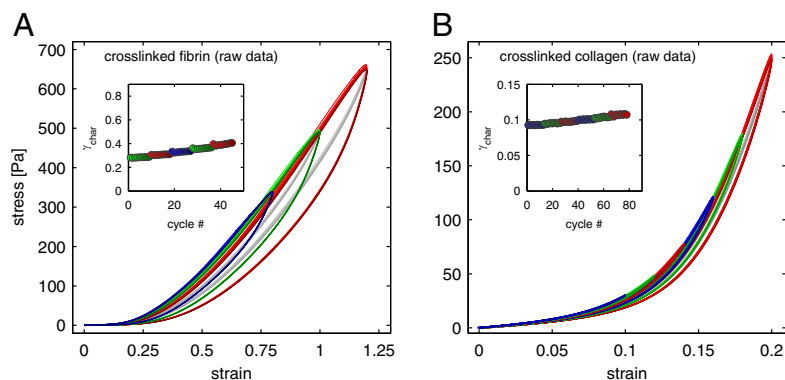


**Fig. 4.** Nonlinear viscoelastic stress response of covalently cross-linked fibrin and collagen networks in response to large-amplitude strain cycles. (A) The stress vs. strain loops of a 1 mg/mL fibrin network cross-linked by factor XIII all overlap and do not display a pronounced shift to larger strains as indicated by the strongly inhibited evolution of  $\gamma_{\text{char}}$  with cycles (*Inset*). (B) The stress response of a 0.9 mg/mL collagen network cross-linked by 0.2% glutaraldehyde displays a similarly suppressed working behavior. (*Inset*) Evolution of  $\gamma_{\text{char}}$  with cycles. (The strain protocols for both systems are identical to those in Fig. 1. The gray lines represent the midlines of the viscoelastic loops from which  $\gamma_{\text{char}}$  is determined for each cycle.)

the strain-stiffening response of the collagen networks occurs at smaller strains and the networks break earlier (Fig. S1C). We therefore adjust the strain amplitudes in our experiment accordingly. In response to repeated straining, the nonlinear response of the collagen network also evolves with every newly imposed cycle (Fig. 1D, same color). When the strain amplitude is increased after 15 oscillations, the network displays an equivalent strain-stiffening response at the higher strains and subsequently undergoes a working behavior (Fig. 1D, different colors). This is consistent with previous work on fibroblast-populated collagen matrices, where uniaxial stretching led to similar responses (32). Once again, we can collapse all recorded stress-strain responses by subtracting an offset strain  $\gamma_{\text{char}}$ , and thereby obtain a single nonlinear master curve as shown in Fig. 1E and F. These data demonstrate that collagen networks also undergo working similar to fibrin networks.

We can also test the influence of covalent cross-linking on collagen networks by an alternative method: We add a solution of 0.2% glutaraldehyde after a network has fully polymerized; glutaraldehyde is a small molecule that can incorporate into protein fibers and covalently binds amino acid residues of neighboring monomers together. Analogous to the fibrin network cross-linked by factor XIIIa, when we repeat our measurements using a collagen network cross-linked with glutaraldehyde, the evolution of the bulk nonlinearity is completely inhibited (Fig. 4B) and each of the loading branches follows the same nonlinear stress-strain response. These findings confirm that covalent cross-linking has a similarly strong effect on the working behavior of collagen networks as it has for fibrin.

## Discussion and Conclusion

In this report, we show that the nonlinear mechanical response of *in vitro* fibrin and collagen networks can change dramatically when these networks are repeatedly strained, provided the intrafibrillar bonds are not permanently cross-linked. This leads to a pronounced working behavior of the network characterized by a shift of the nonlinear stress response to higher strains. We have shown using confocal microscopy that the working of un-cross-linked fibrin networks results from lengthening of individual fibers without altering the network architecture and, thus, the stress-strain response data can be shifted onto a universal master curve when this additional length is subtracted. Because of their similar fiber architecture and rheological response, it is reasonable to expect that fiber lengthening also underlies the mechanical evolution of collagen networks.

Many aspects of this working behavior in un-cross-linked fibrin and collagen networks are also observed in other materials. A weakening of the stress-strain response during repeated straining, known as the “Mullins effect,” is observed for carbon-filled rubbers (33); similar behavior is observed in the “shakedown” of elastomers or hydrogels (34, 35), in the “fluidization” of living cells (36), in the “preconditioning” of tissues (15–18), and in the “dynamic softening” of cross-linked actin biopolymer networks (22, 24). For these materials, however, the mechanical response weakens dramatically between the first and subsequent straining cycles; this finding contrasts with the gradual shift of the entire nonlinear curve to higher strains, which we observe for fibrin and collagen, and which is reminiscent of the preconditioning of collagenous tissues. Furthermore, the underlying mechanisms responsible for strain-induced softening have not been established for the majority of these other materials. By contrast, because we can directly image the individual fibers of fibrin networks using confocal microscopy, we can unambiguously attribute the origin of the behavior in fibrin networks to the lengthening of individual fibers. The only other system for which the underlying mechanism has been identified by direct visualization is reconstituted actin networks; surprisingly, depending on conditions, actin networks exhibit both softening and hardening during cyclic loading. However, the mechanical alterations of actin networks arise

mainly from unbinding and rebinding of cross-linking proteins, combined with structural rearrangements of the network, including fiber bundling, unbinding, or detachment from the plates (22,24).

The gradual working of un-cross-linked fibrin networks results from a successive lengthening of stretched fibers. Such lengthening, or plasticity, at the fiber level is observed in many biopolymer systems, including actin (37), intermediate filaments (38), or microtubules (37), and in the results of molecular dynamics simulations for collagen fibers (39). We demonstrate the consequences of such fiber plasticity on the bulk behavior when these networks are repeatedly strained: Because fibers do not rupture and, thus, the network structure remains unchanged, the shape of the nonlinear response also remains unchanged. Consequently, the data collapse best when shifted through subtraction to scale them onto a master curve. This scaling method is distinct from that commonly used to obtain master curves for other biopolymer networks or living cells (40, 41), where the scaling is achieved through multiplication by a scaling factor. It is possible that scaling through subtraction of a distinct strain may help to describe the data obtained with other materials; this possibility deserves further investigation.

The observed working behavior of fibrin and collagen networks provides a very different material property for a network that is continually subjected to cyclical strain of constant amplitude: Because the individual fibers cannot lengthen beyond their stretched length, the shift of the nonlinear response of the material will be confined to strains at or below the amplitude of the imposed cyclic strain; therefore, the mechanical response of these networks will adapt in such a way that the nonlinearity occurs at this amplitude. In the event of an increase of the strain amplitude, the immediate response will be characterized by a strong nonlinearity of the material; this might help protect the structural integrity of the network by preventing overstretch. This automatic adaptation of the mechanical bulk properties to loading conditions may be a useful design principle for the engineering of bio-inspired materials.

Our results also demonstrate that covalent cross-linking of fibrin and collagen networks controls whether the bulk mechanics of these materials shift under loading or remain fixed. Currently, the two major functions associated with human factor XIII activity are stiffening of the clots and an increase in resilience to lysis (1, 31). We, however, show that factor XIII might also have this third important function of modulating the workability of fibrin. This may have important physiological consequences for blood clots: The complete cross-linking of a blood clot during coagulation takes longer than the formation of its fibrillar backbone (31). Thus, after the initial clot has formed, its mechanical response may be slowly worked by the repeated straining and adapt to the exact mechanical environment; the subsequent cross-linking would then ultimately stabilize these adapted properties and prevent the clot from further working and rupture.

Finally, the influence of cross-linking on the mechanics of collagen may also play a role when living cells migrate through the collagen-rich interstitial space of the ECM during processes such as tissue development, wound healing, or metastasis of cancer. To migrate, cells attach to the fibers of the ECM and create traction forces that propel them (42). These forces put collagen fibers under tension; if the fibers are un-cross-linked, this tension might relax, causing the fibers to lengthen. As a result, un-cross-linked fibers may not be able to support enough tension for the cells to migrate. By contrast, cross-linked fibers may not relax their internal tension as much, thereby supporting traction forces that would facilitate cell migration. Indeed, recent results have implicated covalent cross-linking in tumor progression (43). Hence, not only the stiffening of the ECM caused by the cross-linking of collagen, but also the inhibition of fiber lengthening might play an important role for the increased ability of cancer cells to invade the surrounding ECM. Thus, the full consequences of the working behavior of fibrin and collagen networks remain to be further investigated.

## Materials and Methods

**Polymerization of Fibrin and Collagen Networks.** We dilute human fibrinogen and  $\alpha$ -thrombin (Enzyme Research Labs) in a buffer containing 150 mM NaCl, 20 mM CaCl<sub>2</sub>, and 20 mM Hepes at a pH of 7.4. We create a batch of factor XIII-free fibrinogen by purifying the stock solution as described in the *SI Text*. We polymerize un-cross-linked and cross-linked fibrin networks at 25 °C by mixing 1 vol of 0.4 NIH units/mL thrombin with 1 vol of a 2 mg/mL fibrinogen solution of the factor XIII-free or factor XIII-containing fibrinogen stock, respectively. We quantify the degree of covalent cross-linking by denaturing polyacrylamide gel electrophoresis as described in the *SI Text* and shown in Fig. S6.

For collagen networks, we dilute type I collagen (BD Biosciences) at 4 °C to a final concentration of 0.9 mg/mL in 1× DMEM (Sigma-Aldrich), 25 mM Hepes, and adjust the pH to 9.0 by addition of 1 M NaOH. We initiate polymerization by heating the solution to 25 °C. To covalently cross-link the samples, we pipette a solution of 0.2% glutaraldehyde (Sigma) in 1× PBS (Lonza) around the rheometer geometry once the networks have polymerized for at least 45 min. We incubate the samples for 3 h before performing experiments.

**Rheometry.** We perform all rheological experiments on an ARES-G2 (TA Instruments) strain-controlled rheometer equipped with a 25-mm plate–plate geometry set to a gap of 400  $\mu$ m. For fibrin experiments, we use commercial roughened stainless-steel plates; for collagen experiments, we use a custom-cut 25-mm poly(methyl methacrylate) disk as top plate and a petri dish as the bottom plate. We prevent evaporation by sealing the samples with mineral oil, except for experiments on cross-linked collagen. Here, we use a custom-built solvent trap, which allows for the addition of the cross-linking solution.

We monitor the polymerization of all samples by continuous oscillations with a strain amplitude of 0.005 at a frequency of 1 rad/s. For fibrin samples,

we impose oscillatory cycles at 0.01 Hz in 0.2 strain steps beginning at a strain of 0.4. For collagen samples, we impose cycles at 0.1 Hz in steps of 0.02, beginning at a strain of 0.06. Additional measurements are described in *SI Text*. All data are smoothed with a cubic spline interpolation for plotting.

**Confocal Imaging.** We perform all confocal experiments on a Leica SP5 equipped with a 63 $\times$ /1.2 N.A. water immersion lens. For the confocal strain hold experiment, we polymerize a 1 mg/mL fibrin network from a 1:5 mixture of fibrinogen labeled with 5-(and 6)-carboxytetramethylrhodamine succinimidyl ester (TAMRA-SE) (Invitrogen) and unlabeled fibrinogen in a custom-built shear cell and visualize the full 3D structure with fluorescence confocal scanning microscopy. For single fiber pulling experiments, we create micro-structured channels on a #1 coverslip by imprinting polydimethylsiloxane stamps of ridges (20  $\mu$ m wide, 10  $\mu$ m high) into a drop of Norland Optical adhesive #81 and curing the adhesive in 350-nm UV light. After removal of the stamp, we briefly treat the channels in an oxygen plasma and polymerize unlabeled fibrin networks over them. We remove the majority of the network and visualize the remaining single fibers suspended over the channels by confocal reflection imaging. For fiber manipulation, we sharpen a borosilicate capillary with a commercial capillary puller and coat its tip with PEG-silane to avoid adhesion to the fibers. We mount the capillary onto an Eppendorf Transferman II, which we control via custom software.

**ACKNOWLEDGMENTS.** We thank D. A. Vader, C. P. Broedersz, and F. C. MacKintosh for valuable discussions. This work was supported by the “Emerging Fields Initiative” of the University Erlangen-Nuremberg (Project: TOPBiomat) (to S.M. and B.F.) and by the National Science Foundation through the Harvard Materials Research Science and Engineering Center (DMR-0820484) (to D.A.W.).

- Weisel JW (2004) The mechanical properties of fibrin for basic scientists and clinicians. *Biophys Chem* 112(2–3):267–276.
- Gelse K, Pöschl E, Aigner T (2003) Collagens—structure, function, and biosynthesis. *Adv Drug Deliv Rev* 55(12):1531–1546.
- Wood GC, Keech MK (1960) The formation of fibrils from collagen solutions. 1. The effect of experimental conditions: Kinetic and electron-microscope studies. *Biochem J* 75(3):588–598.
- Ferry JD (1952) The mechanism of polymerization of fibrinogen. *Proc Natl Acad Sci USA* 38(7):566–569.
- Janmey PA, Amis EJ, Ferry JD (1983) Rheology of fibrin clots 6. Stress-relaxation, creep, and differential dynamic modulus of fine clots in large shearing deformations. *J Rheol (N Y N Y)* 27(2):135–153.
- Shah JV, Janmey PA (1997) Strain hardening of fibrin gels and plasma clots. *Rheol Acta* 36(3):262–268.
- Roeder BA, Kokini K, Sturgis JE, Robinson JP, Voytik-Harbin SL (2002) Tensile mechanical properties of three-dimensional type I collagen extracellular matrices with varied microstructure. *J Biomech Eng* 124(2):214–222.
- Storm C, Pastore JJ, MacKintosh FC, Lubensky TC, Janmey PA (2005) Nonlinear elasticity in biological gels. *Nature* 435(7039):191–194.
- Roberts WW, Lorand LL, Mockros LF (1973) Viscoelastic properties of fibrin clots. *Biorheology* 10(1):29–42.
- Nelb GW, Gerth C, Ferry JD, Lorand L (1976) Rheology of fibrin clots. III. Shear creep and creep recovery of fine ligated and coarse unligated clots. *Biophys Chem* 5(3):377–387.
- Hsu S, Jamieson AM, Blackwell J (1994) Viscoelastic studies of extracellular matrix interactions in a model native collagen gel system. *Biorheology* 31(1):21–36.
- Knapp DM, et al. (1997) Rheology of reconstituted type I collagen gel in confined compression. *J Rheol (N Y N Y)* 41(5):971–993.
- Ryan EA, Mockros LF, Weisel JW, Lorand L (1999) Structural origins of fibrin clot rheology. *Biophys J* 77(5):2813–2826.
- Raub CB, et al. (2008) Image correlation spectroscopy of multiphoton images correlates with collagen mechanical properties. *Biophys J* 94(6):2361–2373.
- Fung YC (1993) *Biomechanics: Mechanical Properties of Living Tissues* (Springer, New York), 2nd Ed.
- Schatzmann L, Brunner P, Staubli HU (1998) Effect of cyclic preconditioning on the tensile properties of human quadriceps tendons and patellar ligaments. *Knee Surg Sports Traumatol Arthrosc* 6(Suppl 1):S56–S61.
- Sverdlík A, Lanir Y (2002) Time-dependent mechanical behavior of sheep digital tendons, including the effects of preconditioning. *J Biomech Eng* 124(1):78–84.
- van Dommelen JAW, et al. (2006) Nonlinear viscoelastic behavior of human knee ligaments subjected to complex loading histories. *Ann Biomed Eng* 34(6):1008–1018.
- Fredenburgh JC, Stafford AR, Leslie BA, Weitz JI (2008) Bivalent binding to gammaA/gamma'-fibrin engages both exosites of thrombin and protects it from inhibition by the antithrombin-heparin complex. *J Biol Chem* 283(5):2470–2477.
- Cho KS, Hyun K, Ahn KH, Lee SJ (2005) A geometrical interpretation of large amplitude oscillatory shear response. *J Rheol (N Y N Y)* 49(3):747–758.
- Broedersz CP, et al. (2010) Cross-link-governed dynamics of biopolymer networks. *Phys Rev Lett* 105(23):238101 (lett).
- Wolff L, Fernández P, Kroy K (2012) Resolving the stiffening-softening paradox in cell mechanics. *PLoS One* 7(7):e40063.
- Kabla A, Mahadevan L (2007) Nonlinear mechanics of soft fibrous networks. *J R Soc Interface* 4(12):99–106.
- Schmoller KM, Fernandez P, Arevalo RC, Blair DL, Bausch AR (2010) Cyclic hardening in bundled actin networks. *Nat Commun*, 10.1038/ncomms1134.
- Liu W, Carlisle CR, Sparks EA, Guthold M (2010) The mechanical properties of single fibrin fibers. *J Thromb Haemost* 8(5):1030–1036.
- Liu W, et al. (2006) Fibrin fibers have extraordinary extensibility and elasticity. *Science* 313(5787):634.
- Bale MD, Müller MF, Ferry JD (1985) Effects of fibrinogen-binding tetrapeptides on mechanical properties of fine fibrin clots. *Proc Natl Acad Sci USA* 82(5):1410–1413.
- Shimizu A, Schindlauer G, Ferry JD (1988) Interaction of the fibrinogen-binding tetrapeptide Gly-Pro-Arg-Pro with fine clots and oligomers of alpha-fibrin; comparisons with alpha beta-fibrin. *Biopolymers* 27(5):775–788.
- Brown AEX, Litvinov RI, Discher DE, Purohit PK, Weisel JW (2009) Multiscale mechanics of fibrin polymer: Gel stretching with protein unfolding and loss of water. *Science* 325(5941):741–744.
- Chernysh IN, Nagaswami C, Purohit PK, Weisel JW (2012) Fibrin clots are equilibrium polymers that can be remodeled without proteolytic digestion. *Sci Rep*, 10.1038/srep00879.
- Lorand L (2005) Factor XIII and the clotting of fibrinogen: From basic research to medicine. *J Thromb Haemost* 3(7):1337–1348.
- Wagenseil JE, Wakatsuki T, Okamoto RJ, Zahalak GI, Elson EL (2003) One-dimensional viscoelastic behavior of fibroblast populated collagen matrices. *J Biomech Eng* 125(5):719–725.
- Mullins L (1947) Effect of stretching on the properties of rubber. *Rubber Res* 16:275–289.
- Cantournet S, Desmorat R, Besson J (2009) Mullins effect and cyclic stress softening of filled elastomers by internal sliding and friction thermodynamics model. *Int J Solids Struct* 46(11–12):2255–2264.
- Webber RE, Creton C, Brown HR, Gong JP (2007) Large strain hysteresis and mullins effect of tough double-network hydrogels. *Macromolecules* 40(8):2919–2927.
- Trepat X, et al. (2007) Universal physical responses to stretch in the living cell. *Nature* 447(7144):592–595.
- Kueh HY, Mitchison TJ (2009) Structural plasticity in actin and tubulin polymer dynamics. *Science* 325(5943):960–963.
- Kreplak L, Bär H, Leterrier JF, Herrmann H, Aebi U (2005) Exploring the mechanical behavior of single intermediate filaments. *J Mol Biol* 354(3):569–577.
- Buehler MJ (2006) Nature designs tough collagen: Explaining the nanostructure of collagen fibrils. *Proc Natl Acad Sci USA* 103(33):12285–12290.
- Gardel ML, et al. (2004) Scaling of F-actin network rheology to probe single filament elasticity and dynamics. *Phys Rev Lett* 93(18):188102 (lett).
- Fernández P, Pullarkat PA, Ott A (2006) A master relation defines the nonlinear viscoelasticity of single fibroblasts. *Biophys J* 90(10):3796–3805.
- Friedl P, et al. (1997) Migration of highly aggressive MV3 melanoma cells in 3-dimensional collagen lattices results in local matrix reorganization and shedding of alpha2 and beta1 integrins and CD44. *Cancer Res* 57(10):2061–2070.
- Levental KR, et al. (2009) Matrix crosslinking forces tumor progression by enhancing integrin signaling. *Cell* 139(5):891–906.

# Supporting Information

Münster et al. 10.1073/pnas.1222787110

## Additional Rheometry Experiments

**Rheological Response of an Unworked (“Virgin”) Fibrin Network.** In addition to the repeated large amplitude strain protocol, we measure the nonlinear stress–strain response of a previously unworked (virgin) 1 mg/mL fibrin gel up to a strain of 1. The viscoelastic response of this network is shown in the *Inset* of Fig. S1, black curve.

## Detailed Description of the Rescaling Procedure

Our rescaling procedure consists of three steps: First, we determine the elastic midline  $\sigma_{el}(\gamma)$  of each viscoelastic loop; second, we find the characteristic strain  $\gamma_{char}$  where  $\sigma_{el}(\gamma)$  reaches an arbitrary threshold stress  $\sigma_{thresh}$ , and third, we rescale all of the loops by replotting them so that the differences in the characteristic strains  $\gamma_{char}^i$  are subtracted.

We find the elastic midline of every viscoelastic loop by applying a geometric evaluation of the nonsinusoidal stress response (1, 2). For every strain value  $\gamma_i$  there are two associated stress values: one from the loading curve,  $\sigma_{load}(\gamma_i)$ , and one from the unloading of the material,  $\sigma_{unload}(\gamma_i)$ , as indicated by the arrows in Fig. S2A. The elastic stress  $\sigma_{el}(\gamma_i)$  at each value of  $\gamma_i$  is then constructed as the average of  $\sigma_{load}(\gamma_i)$  and  $\sigma_{unload}(\gamma_i)$ :  $\sigma_{el}(\gamma_i) = (\sigma_{load}(\gamma_i) + \sigma_{unload}(\gamma_i))/2$ . By repeating this for all of the values of  $\gamma_i$  between 0 and the maximum strain of each cycle, the entire curve  $\sigma_{el}(\gamma_i)$  is constructed (Fig. S2A, red line).

After this procedure has been applied to all of the cycles, we determine a characteristic strain  $\gamma_{char}^i$  for each cycle  $i$  as the strain value at which  $\sigma_{el}(\gamma_{char}^i)$  reaches an arbitrarily chosen threshold stress  $\sigma_{thresh}$ , as shown in Fig. S2B by the colored arrows. We determine the difference of  $\gamma_{char}^i$  with  $\gamma_{char}^1$  of the first cycle of each set of oscillations at a given strain amplitude, which we call  $\Delta\gamma_{char}^i = \gamma_{char}^i - \gamma_{char}^1$ .

We obtain the rescaling of our data, as shown in Fig. 1B and E, as follows: We replot all cycles of each set of oscillations at a given amplitude by plotting all stress values  $\sigma_{el}^i(\gamma)$  vs.  $\gamma - \Delta\gamma_{char}^i$ , thus plotting  $\sigma_{el}^i(\gamma - \Delta\gamma_{char}^i)$ . This operation shifts all cycles of a set of oscillations at one strain value on top the first cycle of this set, thereby allowing us to compare their nonlinear shapes, as shown in Fig. S2C. We can also carry out the same operation for the viscoelastic stress–strain raw data (shown in gray in Fig. S2), thereby shifting them accordingly.

We obtain the rescaling of the entire data set for all strain amplitudes onto a single master curve, as shown in Fig. 1C and F, by replotting all stress values  $\sigma_{el}^i(\gamma)$  vs.  $\gamma - \gamma_{char}^i$  and also perform this operation for the viscoelastic raw data.

**Additional Rheological Experiments on an Un–Cross-Linked Fibrin Network with a Cone–Plate Geometry.** In a plate–plate geometry, the strain across the sample increases radially from 0 in the center to maximum strain at the outer edge; hence, all stress values obtained for a particular value of strain are in fact averaged over a mixture of strains. This might influence the results we obtain with a plate–plate geometry. Therefore, to ensure that there is no drawback in using a plate–plate geometry for our purposes, we repeat the exact same series of sinusoidal, large strain oscillations on an un–cross-linked 1 mg/mL fibrin network in the rheometer fitted with a 25-mm/0.0398-rad stainless-steel cone (TA Instruments). A cone–plate geometry exhibits a constant strain profile, therefore resulting in a pure stress measurement over only one value of strain across the entire sample.

The full, symmetric response obtained with the cone–plate geometry is plotted for all cycles in Fig. S3B, side-by-side with

the full response obtained with the plate–plate geometry (Fig. S3A). Both geometries yield nearly identical responses; the response obtained with the cone–plate geometry exhibits slightly larger values for the stress, which is consistent with the uniform strain profile of the cone–plate geometry. However, this might also originate from sample-to-sample variations. Importantly, the resulting viscoelastic cycles show the same shift to larger strains and can be collapsed onto master curves independent of the used geometry, as shown in *Insets* in Fig. S3. This confirms the validity of the data obtained in the plate–plate geometry and demonstrates that there is no qualitative difference.

**Asymmetric Working of Fibrin Network.** In a different experiment, we probe the evolution of the material properties with single-sided sinusoidal strain deformations. We use the “arbitrary wave” function of the rheometer to impose the absolute value of sinusoidal oscillations with a frequency of 0.01 Hz, resulting in a single-sided strain deformation. We increase the strain amplitude of these oscillations in 0.2 strain steps until a strain amplitude of 1 is reached. Subsequently, we apply full sinusoidal strain deformations with an amplitude of 1.2 to probe the full, both-sided material response as shown in the *Upper Inset* of Fig. S4. The response of the material to this protocol is depicted in Fig. S4.

**Stress Relaxation of Fibrin and Collagen Networks.** To probe the stress relaxation of fibrin and collagen networks, we perform a strain hold test after polymerization is completed. We strain the bulk materials with a sudden strain step with an amplitude of 0.4 in case of fibrin, and 0.15 in case of collagen, and monitor the evolution of the resulting stresses over a period of 1 h (Fig. S5).

**Affinity Column Chromatography.** To create a fibrinogen stock free of human factor XIII, we apply commercially available human fibrinogen depleted of plasminogen, von Willebrand factor, and fibronectin (FIB3; Enzyme Research Laboratories) to a FXIII affinity column (anti-FXIII antibody from Affinity Biologicals; CNBr Sepharose from GE Healthcare), precipitate it with ammonium sulfate, and then dialyze it into Tris-saline (20 mM Tris–150 mM NaCl, pH 7.4). We store high-concentration aliquots at  $-80^\circ\text{C}$  until use.

## SDS/PAGE Analysis

We analyze the degree of covalent cross-linking of the resulting fibrin gels using denaturing polyacrylamide gel electrophoresis (SDS/PAGE). We polymerize 1 mg/mL fibrin networks at room temperature by addition of 0.2 NIH units/mL human  $\alpha$ -thrombin. We repeat this procedure on both the original fibrinogen stock containing factor XIII and the stock depleted of factor XIII. We distribute each into aliquots and stop the polymerization/cross-linking reaction after 0, 5, 10, 30, 60, 150 min by addition of 1 vol of Laemmli buffer (Bio-Rad) containing 5% (vol/vol) 2-mercaptoethanol, breaking up the clot by vigorous pipetting, and immediately following this by heating the sample to  $95^\circ\text{C}$  for 3 min.

Once all samples are prepared, we run a 7.5% (wt/vol) polyacrylamide gel containing 0.2% bis-acrylamide under denaturing conditions (running buffer: 0.1% SDS, 0.025 M Tris, 0.192 M glycine) after which we stain the gels with Coomassie blue (Bio-Rad), followed by destaining [10% (vol/vol) acetic acid, 15% (vol/vol) methanol in water]. We load one additional lane with a 10- to 250-kDa protein standard for size comparison (Fig. S6, lane 0).







